Microseismic event detection in noisy environments with instantaneous spectral Shannon entropy

Sérgio Luiz E. F. da Silva and Gilberto Corso

Microseismic event detection in noisy environments with instantaneous-spectral Shannon entropy

Sérgio Luiz E. F. da Silva*
Department of Applied Science and Technology,
Politecnico di Torino, 10129 Torino, Italy and
GISIS, Universidade Federal Fluminense,
Niterói, RJ, 24220-900, Brazil

Gilberto Corso†
Department of Biophysics and Pharmacology,
Federal University of Rio Grande do Norte,
Natal, RN, 59078-970, Brazil

(Dated: July 13, 2022)

The detection of information-bearing signals in a time-series is very important for describing and analyzing a wide variety of complex physical systems. However, identifying events in low signal-to-noise ratio circumstances remains a challenge once heavy data pre-processing is usually required. In this work, we propose a robust methodology based on the instantaneous-spectral Shannon entropy for capturing microseismic events in noisy environments without the requirement of data pre-processing. We call our proposal the Instantaneous Spectral Entropy Detection (ISED) method. We tested the ISED in a couple of real empirical seismic records to detect microseismic events. Our methodology detects microseismic patterns even without any pre-processing, in opposition to usual methods in the literature which need appreciable data pre-processing.

I. INTRODUCTION

The detection and mapping of information-bearing signals is very important in the analysis of physical systems. In recent years, a variety of techniques have been developed to improve the data-transmission quality [1–3] and the low-magnitude signal detection [4–6] for understanding, for instance, the complexity of quantum algorithms [7–9], small movements associated with volcanism [10–12], as well as in biomedical signal analysis [13]. It is worth noting that the extraction of useful information from noisy signals consists in the application of complex approaches that involve sophisticated mathematical, physical and scientific computation techniques. Such a detection task becomes especially difficult when it comes to capturing low-magnitude signals. An example of a low-magnitude signal pattern that is commonly recorded in extremely noisy environments are the microseismic events (or low-magnitude tremors).

The detection of microseismic events is very important for studying the seismicity of a region [14, 15] as well as for understanding the dynamics of several complex systems, such as the rock mass response to mine exploration [16], in reactivation of geological faults [17], in estimation of earthquake-triggering focal mechanisms [18], among many others. However, due to the strong noise scenarios and the low energy of these events, detecting microseismic remains a great challenge. Thus, the scientific community has sought practical solutions for microseismic event detection from time series signals using, for instance, machine learning techniques [19–21] and spectral analysis [22, 23]. In this way, high-quality detecting methodologies are need for a robust microseismic analysis.

Nowadays, the conventional approach for detecting microseismic events is based on the estimation of the average energy of a seismic signal in two moving-time windows, named short-term average (STA) and long-term average (LTA) [24]. The idea behind this framework is to incorporate information that is sensitive both to the seismic event (through the STA window) and to the local seismic noise (through the LTA window). If the ratio between these two time windows (STA/LTA ratio) exceeds a pre-defined value, the existence of an event is declared. Due to its simplicity and effectiveness, the STA/LTA ratio has been widely used for detecting seismic events, for instance, in earthquake early-warning [25] for alerting people about a quake arriving, which allow saving lives from destructive shaking. However, the STA/LTA method is very sensitive to the signal energy, which makes this technique inaccurate for capturing microseismic events recorded in a noisy environment [26].

To improve the detection quality of the classical STA/LTA method in a strong noisy environment, we propose in this work a robust algorithm based on instantaneous spectral Shannon entropy (ISSE) [27], which measures the signal spectral-power distribution in a pre-set time window [28]. The ISSE is useful in biomedical signal analyses [13] and also in fault diagnosis in mechanical systems [28]. Based on the ISSE, we introduce in this work the Instantaneous Spectral Entropy Detection (ISED) method, which is a robust algorithm for capturing seis-

---

* sergio.dasilva@polito.it
† gfcorso@gmail.com

mic waves in noisy environments without pre-processing requirement. In this regard, the ISED is efficient to separate the coherent seismic signal from the noise via information entropy (or Shannon entropy), since there is an increase in the complexity of the spectrogram close to the seismic event signal to be distinguished. In other words, the spectrogram around the seismic event has much more Fourier components compared to the background noise and, as the entropy is a measure of complexity, the ISED reveals a powerful method in this situation.

The outline adopted in this work is as follows. In Sec. II, we start by presenting a brief review of the STA/LTA method, including some examples, from which we illustrate the potential and inability of this classical framework. Then, we present the theoretical foundations and mathematical basis of our proposal: the ISED method. To demonstrate the robustness and effectiveness of our proposal, we consider in Sec. III a real seismic data set of low magnitude natural earthquakes under a very strong background noise. Finally, in Sec. IV, we present the final remarks and perspectives.

II. METHODOLOGY

A. Brief STA/LTA method review

The classical method in seismic event detection, introduced by R.V. Allen in Ref. [24], is the Short Term Average/Long Term Average (STA/LTA) ratio. Let the seismic data consist of N samples: $\mathbf{x} = \{x_1, x_2, ..., x_N\}$, the STA/LTA method consists of calculating the average energy for two time-windows (STA and LTA):

$$\text{STA}_i = \frac{1}{S} \sum_{j=i+1-S}^{i} \text{CF}_j, \tag{1}$$

$$\text{LTA}_i = \frac{1}{L} \sum_{k=i+1-L}^{i} \text{CF}_k, \tag{2}$$

where CF is the so-called characteristic function, S and L are the lengths of a short- and long-term sliding window, and $i = 1, 2, ..., N$. Usually, the CF is defined as an energy function of the signal inside the windows ($CF_j = x_j^2$), absolute value ($CF_j = |x_j|$), envelope function [29], among others [30–32]. If the ratio between the STA, Eq. (1), and LTA, Eq. (2), exceeds a pre-defined threshold, $\frac{STA}{LTA} > \varepsilon$, the existence of a seismic event is declared.

To illustrate the working principle of the classical STA/LTA method, we consider waveforms from two earthquakes: in the first one, an earthquake recorded in Peru-Ecuador-border-region, and in the second one, a tremor recorded in California-Nevada-border-region, see panels (a) and (b) of Fig. 1. We notice that the waveform shown in Fig. 1(a) is less contaminated by noise than the

waveform shown in Fig. 1(d). By considering data length (sample size) in the short-term sliding window set up to $S = 4s$ and long-term to $L = 24s$, the respective STA and LTA series are constructed using Eqs. (1) and (2), as depicted in panels (c) and (d) of Fig. 1. With the STA [green (light gray) curve in Figs. 1(b) and 1(e)] and LTA series [blue curve in Figs. 1(b) and 1(e)], the STA/LTA ratio is computed [see Figs. 1(c) and 1(f)]. If we consider the threshold factor to be $\varepsilon = 2$, for example, we observe that STA/LTA method correctly identifies the earthquake in Peru-Ecuador-border-region [see Fig. 1(c)], but fails to capture the earthquake in California-Nevada-border-region [see Fig. 1(f)]. In fact, STA/LTA method is only successful when the signal has a high signal-to-noise ratio (SNR), which is not the case for microseisms in areas subject to strong background noise like those close to urban activities [33].

B. Instantaneous Spectral Entropy Detection (ISED)

Based on the theory of information, C. Shannon [34] introduced the mathematical bases and foundations of communication theory, in which the characterization of information measures are analyzed using the so-called Shannon entropy. In the last years, Shannon entropy has been applied in several areas of the science, such as statistical physics [35–37], information theory [38, 39], inference problems [40, 41], among many others. Formally, for a set of measures $x_1, x_2, \cdots, x_n$, Shannon entropy provides a number that represents the uncertainty measure, or degree of complexity, associated with a given probability distribution $p(x)$. This entropy is written as the following functional:

$$\mathcal{H}[p] = -\sum_{i=1}^{n} p(x_i) \ln \left(p(x_i) \right). \tag{3}$$

In this work, we take into account the fact that the signal amplitudes x computed into the signal-window and the k-th frequency f_k are given by an instantaneous probability function $p(t, f_k)$. In this regard, the Instantaneous Spectral Shannon Entropy (ISSE) is defined as [27, 42]:

$$\mathcal{H}(t) = -\sum_{k} p(t, f_k) \ln \left(p(t, f_k) \right), \tag{4}$$

where $p(t, f_k)$ computes the instantaneous probability function linked with the time-frequency power-spectrum $\mathbb{S}(t, f_k)$ as follows:

$$p(t, f_k) = \frac{\mathbb{S}(t, f_k)}{\sum_j \mathbb{S}(t, f_j)}. \tag{5}$$

It is worth noting that the entropic functional in Eq. (4) is computed at each time window using the time-frequency power spectrogram, and t represents the average value of that time-window. Furthermore, we notice that the
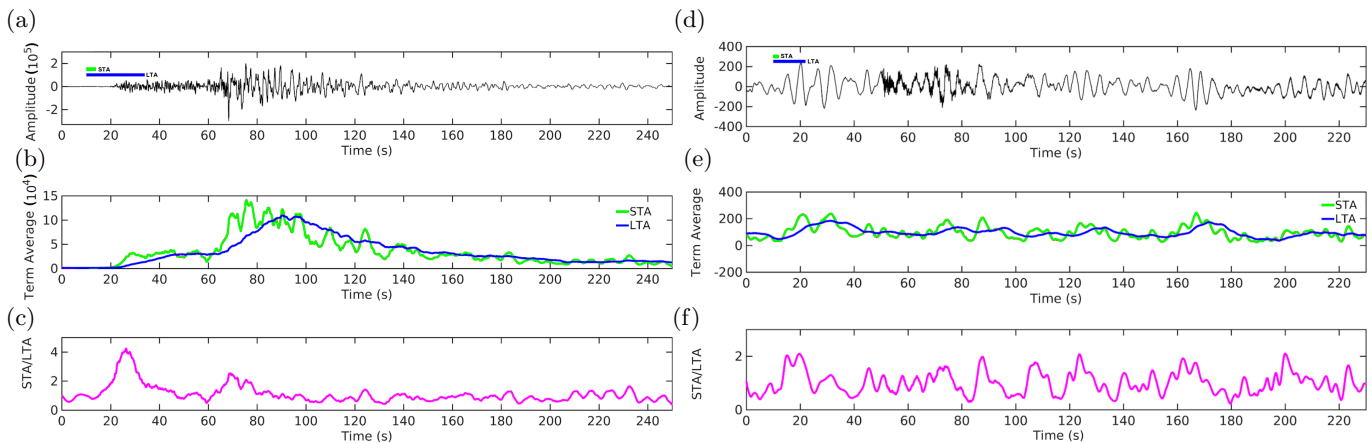
FIG. 1. A simple example to illustrates the STA/LTA method. (a) Waveform recorded at 2019-03-20 in Peru-Ecuador-border-region. (b) STA (green (light gray) curve) and LTA (blue curve) series by considering 4 and 24 seconds of time-windows lengths. (c) STA/LTA ratio. (d) A low magnitude natural earthquake to illustrate the limitations of the STA/LTA method, which is a waveform recorded at 2019-06-27 in California-Nevada-border-region. In addition, panel (e) depicts the STA and LTA series using a 4 and 24 seconds for computing the time-windows lengths and panel (f) shows the corresponding STA/LTA ratio.

ISSE, Eq. (4), provides a measure of the homogeneity of the frequency contents for each time-window, revealing peaks in times of the most energy-containing time-windows [27]. In this way, it is expected that the noise energy spread out through the spectrum. Thus, the peaks in the ISSE series must correspond to seismic events, as will be shown below.

Since the noise spreads out and the coherent information (i.e., the microseismic event) concentrates in some areas of the spectrogram, the ISSE should be greater in the region referred to the microseismic event (that has greater energy in the time-frequency power-spectrum regarding the noise) than the background noise at each time instant. In this regard, we propose a robust methodology based on the ISSE for detecting low-energy signals in very noisy environments for unfiltered data. Thus, our proposal called Instantaneous Spectral Entropy Detection (ISED) is able to identify (micro)seismic events in a long time series, even when it is polluted by a strong background noise, without the requirement for data pre-processing. Moreover, the independence of pre-processing make this tool relevant in automated projects.

We divide the ISED method into three main steps: in the first one, we compute the signal time-frequency power-spectrum using the windowed Fourier transform and calculate the instantaneous probability at each time window considering their respective spectral contents. Second, we compute the ISSE by automatically generating a new time series associated with the Shannon entropy of the spectral content of each time-window. Finally, the ISSE time-series is employed as input to the STA/LTA method for automatic detection of the peak of the ISSE which is related to the seismic events. We summarize our proposal ISED procedure in Fig. 2.

III. MICROSEISMIC DETECTION CASE STUDY

To test the robustness and effectiveness of the ISED technique, and empirically validate our proposal, we employ a real data set obtained from *Incorporated Research Institutions for Seismology* (IRIS) [43]. The data set consists of waveforms of seismic events recorded in three different regions, as summarized in Table I. It is worth noting that the seismic records used in this work were registered by several institutions that collaborate with IRIS University Consortium. The event #01 was recorded near the coast of Peru at the Nana station (NNA) located in Peru [latitude 11.99° S and longitude 76.84° W]. The events #02 and #03 were recorded in the United States of America (USA) by the Columbia College station (CMB) [located in Columbia, CA: latitude 38.03° N and longitude 120.39° W] and NVAR Array Site 31 station (NVAR) [located in Mina, NV: latitude 38.43° N and longitude 118.16° W].

We consider in the first detection test the waveform of the event #01 [see Table I]. In particular, we extract the waveform from the vertical channel of the NNA station, which is depicted in Fig. 3(a). In this figure, the green and magenta color lines represent the detection of P and S-waves performed automatically by the classical STA/LTA method, whilst the green and blue color lines represent the detection of P and S-waves performed automatically by the ISED method. To apply the ISED technique, we compute the ISSE, Fig. 3(c), from the time-frequency power spectrogram depicted in Fig. 3(b). The travel-time estimated are represented by the green and blue color lines. As expected, the spectrogram region referring to the seismic event is more strongly represented, as depicted by the colors close to green in Fig. 3(b), than the region from the background noise. Note that, as
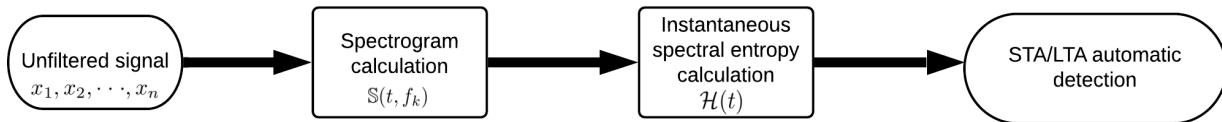
FIG. 2. Flowchart summarizing our proposal to the robust automatic seismic event detection, which dispenses the requirements to a data pre-processing.

Event ID	Region name	Date (yyyy/mm/dd)	Time UTC (hh:mm:ss)	Latitude (°)	Longitude (°)	Depth (km)	Magnitude
01	Coastal region of Peru	2019/03/22	12:50:30	12.64° S	76.59° W	48.14	4.6 m_b
02	Columbia, CA, USA	2019/03/23	07:34:18	37.30° N	117.50° W	7.0	3.0 m_l
03	Mina, NV, USA	2019/06/27	17:00:07	37.23° N	117.68° W	0.96	1.9 m_l

TABLE I. Main information on the earthquakes, used in this study, extracted from the IRIS University Consortium [43] which consists of earthquake's date, time, hypocentral location, and magnitude.

expected, the STA/LTA algorithm with or without the ISSE successfully identified the P- and S-wave arrivals, since the event #01 is not very strongly contaminated by noise.

In contrast to the previous seismic signal, the last two seismic data have a low signal-to-noise ratio, which difficult the P- and S-waves detection, see panel (a) of Figs. 4 and 5. In these two cases, the classical STA/LTA algorithm was unable to identify the P- and S-waves from the unfiltered signals recorded in the vertical channel of CMB and NVAR stations [events #02 and #03]. In fact, in these two situations, the amplitude of the background noise is of the same order of magnitude as the seismic events. On the other hand, our proposal was able to identify the P- and S-waves, the positions are represented by the red and blue bars in Figs. 4 and 5. Such success is due to the spread out of background noise energy through the spectrogram and the concentration of the seismic event energy. The strong energy of the seismic events are visualized by colors close to red in the spectrograms [Figs. 4(b) and 5(b)]. In this regard, ISSE has remarkable maximum points [Figs. 4(c) and 5(c)], which helps the STA/LTA algorithm to identify seismic events even under adverse circumstances.

To validate our results, we process the seismograms in Figs. 4 and 5 with the Seismic Analysis Code (SAC) [44, 45] by: (i) removing the mean of the signal; (ii) applying a symmetric Hanning taper; and (iii) filtering the signal between 2 and 20 Hz using a Butterworth filter. The processed waveforms are shown in panel (d) of Figs. 4 and 5, where the P- and S-waves are clearly visible. Using the filtered data, both methodologies are able to automatically identify P- and S-waves. Therefore, the processed signals validates that our methodology does not require a pre-processing to correctly identify the microseismic events from a low signal-to-noise ratio recorded data.

IV. FINAL REMARKS

In this work, we have introduced a robust methodology for detecting low-magnitude tremor events in (strong) noisy environments using the instantaneous-spectral Shannon entropy. Since many physical systems are characterized by information-bearing microsignals in low signal-to-noise ratio circumstances, a long (and, sometimes, a tedious) data pre-processing is required for starting the physical analyses. In this way, our proposal mitigates the requirement of a data pre-processing, which is useful for analyzing large data sets and using automatic methodologies as those applied in machine learning, for instance. We call our proposal the Instantaneous Spectral Entropy Detection (ISED) method.

Since the ISED is based on the assumption that the energy of the background noise is spread out in the spectrogram, we compute the Shannon entropy for each time-frequency power-spectrum of the signal in order to identify the maximum entropy associated with the microseismic event. Applications of our proposal in real data sets demonstrated the potentialities of the ISED to identify information-bearing signals in a very noisy scenario, which indicates that the ISED is an effective methodology for automatic detecting microseismic events recorded under strong background noise. In fact, our proposal was able to successfully identify the presence of low-magnitude seismic waves obscured by noise. In this way, we believe that the ISED is a strong alternative for analyzing large-scale multichannel datasets.
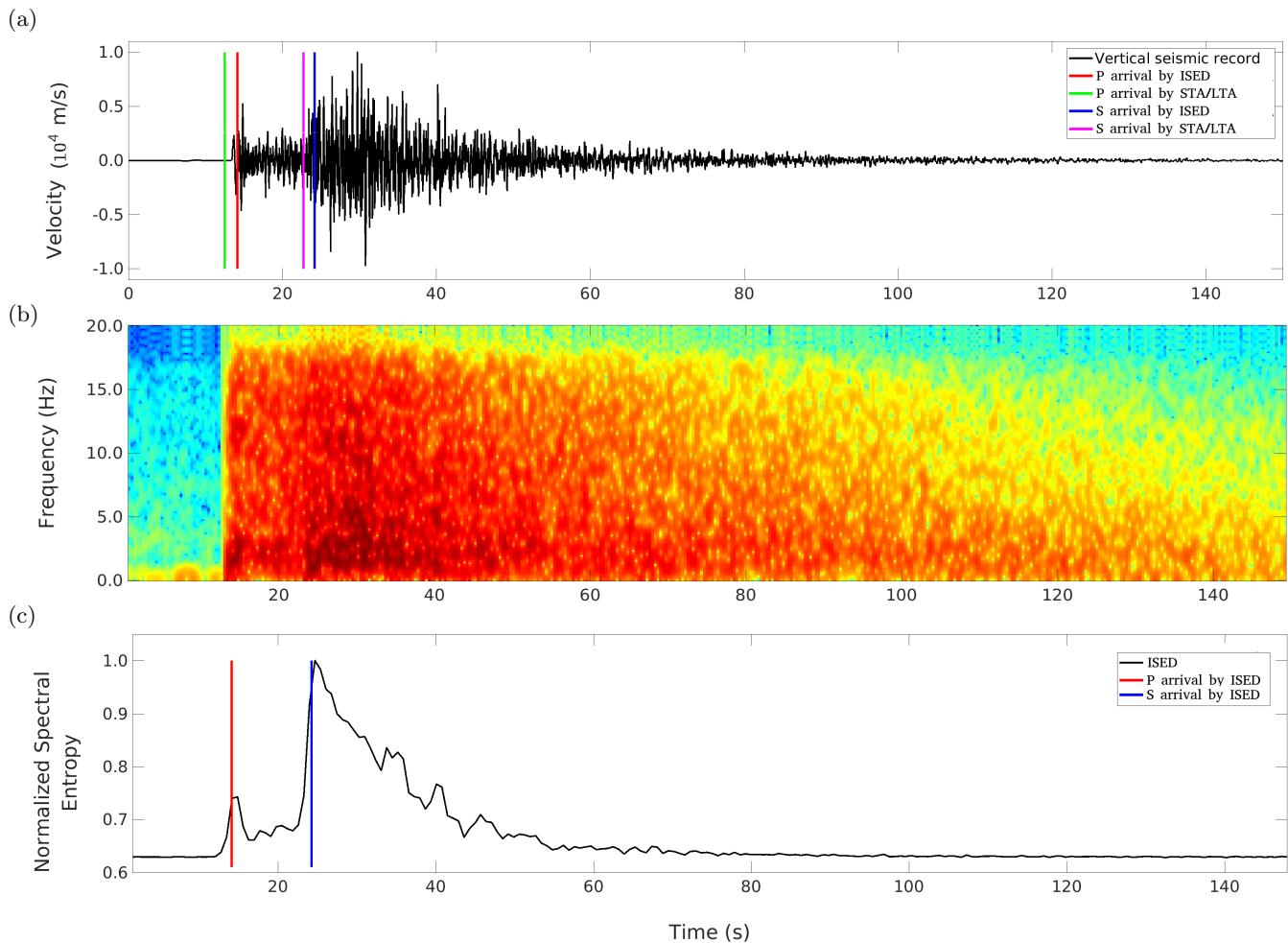
V. ACKNOWLEDGEMENTS

(a)

(b)

(c)

FIG. 3. (a) Unfiltered waveform of the event #01 and (b) its respective time-frequency power-spectrum. Panel (c) depicts the ISSE associated with the event #01. In panels (a) and (c), the colored vertical lines represent the identification of the P- and S-waves for each method.

[1] F. Liu, J. Feng, and W. Wang, Impact of poisson synaptic inputs with a changing rate on weak-signal processing, EPL **64**, 131 (2003).

[2] M. V. Ribeiro, J. M. T. Romano, and C. A. Duque, An improved method for signal processing and compression in power quality evaluation, IEEE Trans. Power Deliv. **19**, 464 (2004).

[3] J. Wang and Z. Liu, A chain model for signal detection and transmission, EPL **102**, 10003 (2013).

[4] S. J. Gibbons and F. Ringdal, The detection of low magnitude seismic events using array-based waveform correlation, Geophys. J. Int. **165**, 149 (2006).

[5] R. G. T. Mello, L. F. Oliveira, and J. Nadal, Digital butterworth filter for subtracting noise from low magnitude surface electromyogram, Comput. Methods Programs Biomed. **87**, 28 (2007).

[6] J. Fu, X. Wang, Z. Li, H. Meng, J. Wang, W. Wang, and C. Tang, Automatic phase-picking method for detecting earthquakes based on the signal-to-noise-ratio concept, Seismol. Res. Lett. **91**, 334 (2019).

[7] Y. C. Eldar and A. V. Oppenheim, Quantum signal processing, IEEE Signal Process. Mag. **19**, 12 (2002).

[8] G. H. Low and I. L. Chuang, Optimal hamiltonian simulation by quantum signal processing, Phys. Rev. Lett. **118**, 010501 (2017).

[9] D. Belkic, *Quantum-Mechanical Signal Processing and Spectral Analysis. In: Series in Atomic Molecular Physics* (CRC Press, 2019).

[10] M. Bohnhoff, M. Rische, T. Meier, D. Becker, G. Stavrakakis, and H. P. Harjes, Spatio-temporal microseismicity clustering in the cretan region, Tectonophysics **423**, 17 (2007).
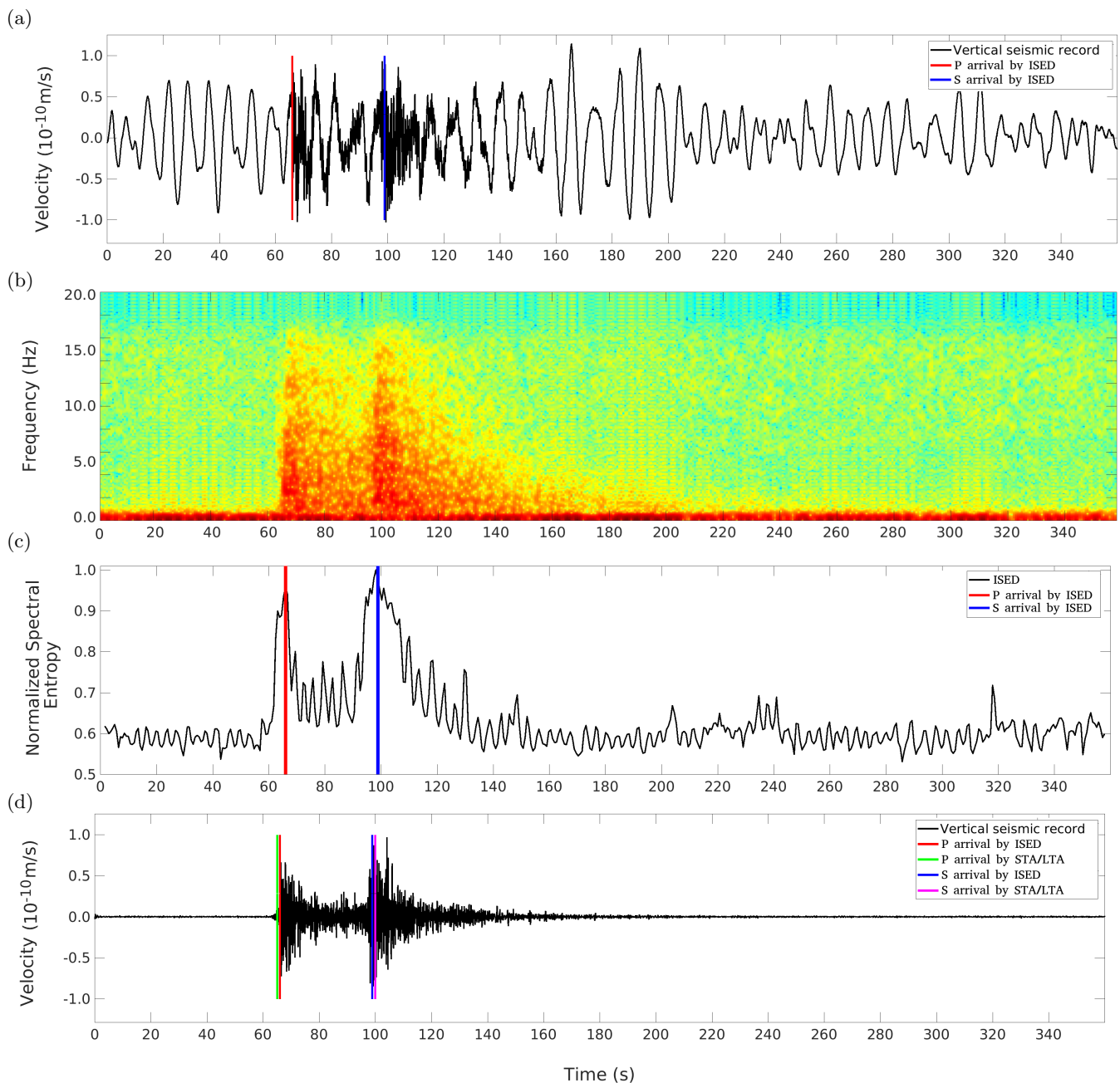
FIG. 4. (a) Unfiltered waveform of the event #02 and (b) its respective time-frequency power-spectrum. Panel (c) depicts the ISSE associated with the event #02 and panel (d) depicts the pre-processed waveform. The colored vertical lines represent the identification of the P- and S-waves for each method.

[11] T. Cladouhos, S. Petty, Y. Nordin, M. Moore, K. Grasso, M. Uddenberg, M. Sawyer, B. Julian, and G. R. Foulger, *Microseismic monitoring of Newberry volcano EGS demonstration. In: 38th Workshop on Geothermal Reservoir Engineering 2013* (Curran Associates, 2013).

[12] J. Li, L. Stankovic, S. Pytharouli, and V. Stankovic, Automated platform for microseismic signal analysis: Denoising, detection, and classification in slope stability studies, IEEE Trans. Geosci. Remote Sens. **59**, 7996 (2021).

[13] A. Vakkuri, A. Yli-Hankala, P. Talja, S. Mustola, H. Tolvanen-Laakso, T. Sampson, and H. Viertiö-Oja,

Time-frequency balanced spectral entropy as a measure of anesthetic drug effect in central nervous system during sevoflurane, propofol, and thiopental anesthesia, Acta Anaesthesiol. Scand. **48**, 145 (2004).

[14] M. Ashtari, D. Hatzfeld, and N. Kamalian, Microseismicity in the region of tehran, Tectonophysics **395**, 193 (2005).

[15] D. Schorlemmer and S. Wiemer, Microseismicity data forecast rupture area, Nature **434**, 1086 (2005).

[16] J. Julià, A. A. Nyblade, R. Durrheim, L. Linzer, R. Gök, P. Dirks, and W. Walter, Source mechanisms of mine-related seismicity, savuka mine, south africa, Bull. Seis-
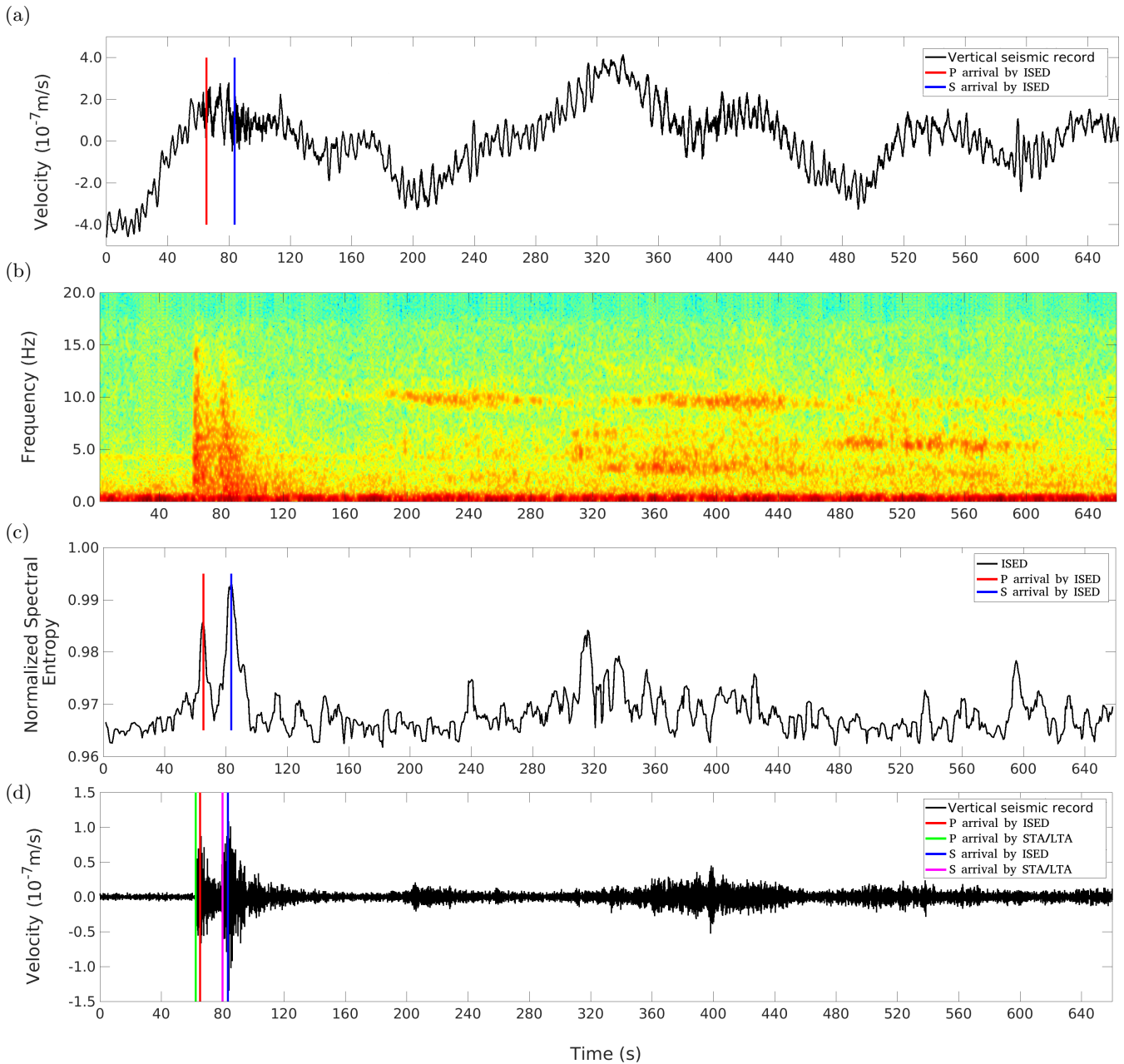
FIG. 5. (a) Unfiltered waveform of the event #03 and (b) its respective time-frequency power-spectrum. Panel (c) depicts the ISSE associated with the event #03 and panel (d) depicts the pre-processed waveform. The colored vertical lines represent the identification of the P- and S-waves for each method.

mol. Soc. Am. **99**, 2801 (2009).

[17] H. C. Lima Neto, J. M. Ferreira, F. H. R. Bezerra, M. S. Assumpção, A. F. do Nascimento, M. O. L. Sousa, and E. A. S. Menezes, Upper crustal earthquake swarms in são caetano: Reactivation of the pernambuco shear zone and trending branches in intraplate brazil, Tectonophysics **608**, 804 (2013).

[18] S. L. E. F. da Silva, J. Julià, and F. H. Bezerra, Deviatoric moment tensor solutions from spectral amplitudes in surface network recordings: Case study in são caetano, pernambuco, brazil, Bull. Seismol. Soc. Am. **107**, 1495 (2017).

[19] Y. Wu, Y. Lin, Z. Zhou, D. C. Bolton, J. Liu, and P. Johnson, Deepdetect: A cascaded region-based densely connected network for seismic event detection, IEEE Trans. Geosci. Remote Sens. **57**, 62 (2019).

[20] S. Qu, Z. Guan, E. Verschuur, and Y. Chen, Automatic high-resolution microseismic event detection via supervised machine learning, Geophys. J. Int. **222**, 1881 (2020).

[21] A. Othman, N. Iqbal, S. M. Hanafy, and U. B. Waheed, Automated event detection and denoising method for passive seismic data using residual deep convolutional neural networks, IEEE Trans. Geosci. Remote Sens. **60**,

1 (2022).

[22] J. Kortström, M. Uski, and T. Tiira, Automatic classification of seismic events within a regional seismograph network, Comput. and Geosci. **87**, 22 (2016).

[23] J. Fu, X. Wang, Z. Li, H. Meng, J. Wang, W. Wang, and C. Tang, Automatic Phase-Picking Method for Detecting Earthquakes Based on the Signal-to-Noise-Ratio Concept, Seismol. Res. Lett. **91**, 334 (2019).

[24] R. V. Allen, Automatic earthquake recognition and timing from single traces, Bull. Seismol. Soc. Am. **68**, 1521 (1978).

[25] A. Lomax, C. Satriano, and M. Vassallo, Automatic picker developments and optimization: Filterpicker—a robust, broadband picker for real-time seismic monitoring and earthquake early warning, Seismol. Res. Lett. **83**, 531 (2012).

[26] A. Trnkoczy, Understanding and parameter setting of sta/lta trigger algorithm (*In:* IASPEI New Manual of Seismological Observatory Practice, 2002).

[27] U. Melia, F. Claria, M. Vallverdu, and P. Caminal, Measuring instantaneous and spectral information entropies by shannon entropy of choi-williams distribution in the context of electroencephalography, Entropy **16**, 2530 (2014).

[28] Y. N. Pan, J. Chen, and X. L. Li, Spectral entropy: A complementary index for rolling element bearing performance degradation assessment. *In*: Proceedings of the institution of mechanical engineers (J. Mech. Eng. Sci., 2009) p. 1223.

[29] P. S. Earle and P. M. Shearer, Characterization of global seismograms using an automatic-picking algorithm, Bull. Seismol. Soc. Am. **84**, 366 (1994).

[30] J. I. Sabbione and D. Velis, Automatic first-breaks picking: New strategies and algorithms, Geophysics **75**, V67 (2010).

[31] A. Khalqillah, M. Isa, and U. Muksin, A gui based automatic detection of seismic p-wave arrivals by using short term average/long term average (sta/lta) method, J. Phys.: Conf. Ser. **1116**, 032014 (2018).

[32] X. Longjun and C. Yabin, Easy detection for the high-pass filter cut-off frequency of digital ground motion record based on sta/lta method: a case study in the 2008 wenchuan mainshock, J. Seismol. **25**, 1281 (2021).

[33] S. T. R. Maciel, M. P. Rocha, and M. Schimmel, Urban seismic monitoring in brasília, brazil, PLOS ONE **16**, e0253610 (2021).

[34] C. E. Shannon, A mathematical theory of communication, Bell Syst. Tech. J. **27**, 379 (1948).

[35] L. Ponta and A. Carbone, Information measure for financial time series: Quantifying short-term market heterogeneity, Physica A **510**, 132 (2018).

[36] A. Jurgens and J. Crutchfield, Shannon entropy rate of hidden markov processes, J. Stat. Phys. **183**, 32 (2021).

[37] C. Edet and A. Ikot, Shannon information entropy in the presence of magnetic and aharanov–bohm (ab) fields, Eur. Phys. J. Plus **136**, 432 (2021).

[38] J. Lin, Divergence measures based on the shannon entropy, IEEE Trans. Inf. Theory **37**, 145 (1991).

[39] L. Telesca, V. Lapenna, and M. Lovallo, Information entropy analysis of seismicity of umbria-marche region (central italy), Nat. Hazards Earth Syst. Sci. **4**, 691 (2004).

[40] S. L. E. F. da Silva, P. T. C. Carvalho, C. A. N. da Costa, J. M. de Araújo, and G. Corso, Misfit function for full waveform inversion based on shannon entropy for deeper velocity model updates (*In:* SEG Technical Program Expanded Abstracts. Society of Exploration Geophysicists, Houston, Texas, USA, 2009) pp. 1556–1559.

[41] A. Posadas, J. Morales, and A. Posadas-Garzon, Earthquakes and entropy: Characterization of occurrence of earthquakes in southern spain and alboran sea, Chaos **31**, 043124 (2021).

[42] A. M. Fraser and H. L. Swinney, Independent coordinates for strange attractors from mutual information, Phys. Rev. A **33**, 1134 (1986).

[43] IRIS Earthquake Browser, IRIS - Incorporated Research Institutions for Seismology *http://www.ds.iris.edu* , Last accessed: 05 January 2021 (2021).

[44] P. Goldstein, D. Dodge, M. Firpo, and L. Minner, Sac2000: Signal processing and analysis tools for seismologists and engineers (*In:* The IASPEI International Handbook of Earthquake and Engineering Seismology, Edited by WHK Lee, H. Kanamori, P.C. Jennings, and C. Kisslinger, Academic Press, London., 2003).

[45] P. Goldstein and A. Snoke, Sac availability for the iris community (Incorporated Institutions for Seismology Data Management Center Electronic Newsletter, 2011).